Topological properties of interfacial hydrogen bond networks

Ruiyu Wang[1,2], Mark DelloStritto[3], Michael L. Klein[1,2,3], Eric Borguet[1,2],* and Vincenzo Carnevale[3,4]†
[1]*Department of Chemistry, Temple University, Philadelphia, Pennsylvania 19122, United States*
[2]*Center for Complex Materials from First Principles (CCM), Temple University, 1925 North 12th Street, Philadelphia, Pennsylvania 19122, United States*
[3]*Institute for Computational Molecular Science, Temple University, Philadelphia, Pennsylvania 19122, United States*
[4]*Department of Biology, Temple University, Philadelphia, Pennsylvania 19122, United States*
(Dated: June 6, 2024)

Hydrogen bonds play a crucial role in the anomalous behavior of water. While the properties of individual H-bonds have been extensively studied, the topological characteristics of the resulting H-bond network remain less explored. In this study, we employ molecular dynamics simulations to examine various aqueous interfaces, uncovering an increased number of H-bonds parallel to surfaces compared to bulk water. To quantify the topology of these networks, we introduce novel estimators for network percolation and dimensionality. Our findings reveal that the elevated proportion of H-bonds parallel to the interface significantly influences network connectivity, reducing both the number of water layers and the distance from the surface at which the network achieves full connectivity. Consequently, H-bond networks at interfaces exhibit more "two-dimensional" characteristics than those in bulk water due to high local water density and the competition between water-water H-bonds and water-surface interactions.

INTRODUCTION

Understanding and controlling interfacial phenomena is essential for a wide range of applications, including catalysis, electrochemistry, dissolution, corrosion, and electrochemical energy storage[1–9]. A fundamental question about interfacial phenomena concerns the origin of their distinct properties: how do these properties depend on the structure of the solid and liquid components? The question is especially pertinent for aqueous interfaces, as strong hydrogen bonds (H-bonds) of water result in a structured liquid with anomalous behaviors, such as a high boiling point and surface tension[10, 11]. The fluctuation of H-bonds also play a critical role in driving proton transfer in water[12–18].

In bulk water, each water molecule forms an average of 3.5 H-bonds[19], much higher than the percolation threshold of a 3D network[20]. This suggests the presence of an isotropic and homogeneous H-bond network connecting all waters without a preferred orientation[21–23]. However, H-bond networks at interfaces often differ substantially from those in bulk water[1]. For instance, at the water/air interface, the vacuum allows free unbonded OH groups to be perpendicular to the surface and point toward to the air[24–26]. H-bonds between interfacial waters tend to be parallel to the surface, resulting in a connected H-bond network at the topmost layer of the interface[27–29]. Besides planar surfaces, water/protein interfaces exhibit a monolayer of protein hydration that displays "quasi-2D percolation", a phenomenon believed to be related to proteins' biofunctions[30–32].

Previous research has focused on individual H-bonds[33] and their perturbation by solute molecules[24]. However, quantitative descriptions for the entire H-bond network at interfaces are missing. To compare the entire network at different interfaces and differentiate it from bulk water, we proposed universal network descriptors using graph based approaches to characterize the 2D density-dependent connectivity of water at water/air, α-alumina(0001), modified graphene, Pt(111) surfaces and the cut-bulk surface [34–39] (defined in the Supporting Information, SI [40]). These surfaces are charge neutral, possessing both hydrophilic and hydrophobic character. Interfacial waters interact strongly with the alumina surface but weakly with all other surfaces[41–43]. The modified graphene surface contains alternative positive and negative charges on the carbon atoms, showing both hydrophilic and hydrophobic behaviors[44]. Simulation results demonstrate that interfacial water H-bond networks are more densely connected than those in bulk water. Although this property holds true for all surfaces, we observe quantitative variations stemming from the hydrophilicity of surfaces and the local water density.

To comprehensively investigate the nature of an interface, it is imperative to accurately define its dimension. This task is challenging especially for liquid-liquid interfaces and liquid-vapor interfaces that often exhibit intricate shapes with ambiguously delineated boundaries. To estimate the dimensionality of the interface it is necessary to develop a method to estimate the dimensionality of an arbitrary arrangement of molecules. One effective strategy is to take advantage of the scaling laws, where the intrinsic dimension of the space is deduced from the limit of the cumulative distribution of pair distances as the distance approaches zero[45]. Unfortunately, complex manifolds of points and noise can cause problems with the estimation of the dimension[46]. An alternative approach is to compute the intrinsic dimension of a set of points by using the geodesic distances, which measures the length of the pathways between points using only nearest-neighbor graph distances. This method yields accurate intrinsic dimensions regardless of the shape of

the manifold of points[46]. Consequently, the approach can be employed to assess the intrinsic dimension of a molecule set situated at an interface.

While measuring the intrinsic dimension of a molecular system is an excellent technique to determine its overall shape, the structure of the H-bond network is ignored. Methods to measure the intrinsic dimension work on a series of points in N dimensions. In the context of water, these points correspond to the positions of the water molecules, defined by the positions of the oxygen (O) atoms. As each water molecule frequently both accepts and donates H-bonds to its neighbors, water can be treated as a dynamic percolation network. An alternative strategy to assess the structure of an aqueous interface involves investigating the connectivity of interfacial water and the path of their H-bond network.

Anticipating our results, we find that we can accurately measure the change of dimension of interfacial water using the intrinsic dimension, defined as the dimension of a minimal representation of a molecular structure. While there are small deviations in the intrinsic dimension between interfaces, the dimension shows similar behavior for all interfaces, and can take several nanometers to converge to bulk values.

The connectivity of an H-bond network at interfaces generally yields more information than the dimensionality. While 2D densities are the same at the surfaces investigated in this work, the interfacial H-bond network has higher connectivity than that of bulk water. The size of connected components formed by the H-bond networks are very different for different interfaces, illustrating the importance of the competition between interactions, which defines interfacial behaviors.

RESULTS AND DISCUSSIONS

Intrinsic dimensions of interfacial water

It is important to determine whether the width of the interfacial region differs between various interfaces with different materials. We identify the location and thickness of the interfaces using the dimensionality, that is, where the bulk liquid ends, and the interfacial region begins. We measure the size of the interface by computing the intrinsic dimension of the interface as a function of depth from the point at which the density drops below $10^{-6}\ nm^{-3}$. The intrinsic dimension can be thought of as the dimension of a minimal description for a set of data. To make this idea more concrete, when applied to structures, the intrinsic dimension can be thought of as the fewest number of dimensions required to specify all points of the structure. For example, consider a sheet of graphene and a carbon nanotube, where it might at first appear that the two structures have different dimensions. The graphene sheet is flat and fits in a 2D plane and thus has a dimension of 2, while on the other hand the carbon nanotube has a width, height, and length and thus would appear to have a dimension of 3. However, note that both structures can be fully described using only 2 variables: the graphene sheet by the x-y displacement, and the carbon nanotube by the angular and longitudinal displacement. Thus, while the sheet and the tube require a different number of Cartesian dimensions, their intrinsic dimension is the same. One can define the intrinsic dimension for any set of points using a graph distance approach[46]. We use this method to obtain the intrinsic dimension of a group of water molecules by using the Oxygen positions as the inputs for the intrinsic dimension estimator.

As expected, the intrinsic dimension as a function of depth (Fig. 1) for interfaces between water and a range of different materials rises from an initial value of approximately 2 to an asymptotic value of approximately 3 over a distance of about 3 nm, which matches the thickness of interfaces inferred from density fluctuations[47]. While there are some slight differences between the profiles of different interfaces, they overall exhibit a remarkable similarity. This is particularly surprising for the more flexible air/water interface, which has some fluctuations out of the plane of the interface, in contrast to interfaces with rigid bulk materials like alumina and platinum. Thus, while the dimensionality of the interface is well defined and reproduces results from other measures of the interface, it does not yield any insight into the nature of the H-bond network at various interfaces. This is most likely because the intrinsic dimension of a set of points is defined by graph distances without any directionality, and this ignores the directional nature of the H-bonds between water molecules.

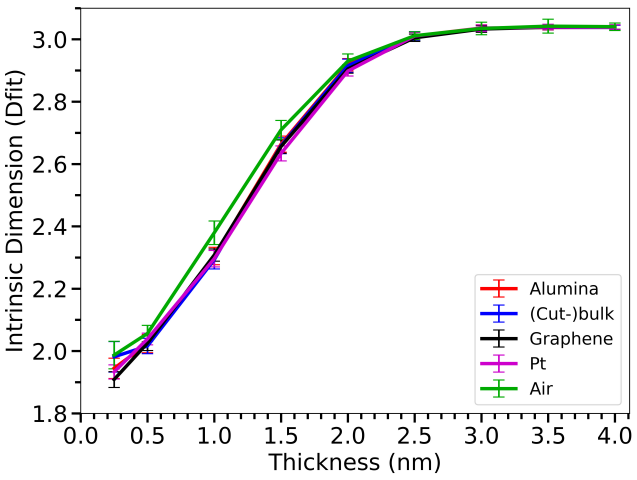

FIG. 1. Plot of the intrinsic dimension of different water interfaces as a function of the depth of the interface from the point of zero density.

Density and orientation of hydrogen bonds between interfacial waters

A perfect, isolated 2D H-bond network requires that all water molecules reside within the same plane, akin to the structure of 2D ice[48–50]. The configuration gives rise to a δ-like function representing the local density of water oxygen atoms. However, in this work, such an ideal, well-structured arrangement has not been observed. Only at the Pt surface, water density between the first two peaks is close to 0. The density of this region at graphene and alumina surface is reduced but still higher than 0. The first peak of the local water density is significantly higher than the bulk liquid at alumina, Pt(111) and graphene surfaces, suggesting a possible competition between H-bonds parallel and perpendicular to the surface. As for the cut-bulk, the reference system with 3D behavior, the density profile shows no pronounced peaks. Since the distance between two peaks of water local density at Pt surface is less than 0.3 nm and H-bonds between the two layers still persist, interfacial H-bond network is not isolated from bulk waters. Nevertheless, it is inadequate to conclude that the water H-bond network at Pt surfaces shows 2D behavior based on water density profile only.

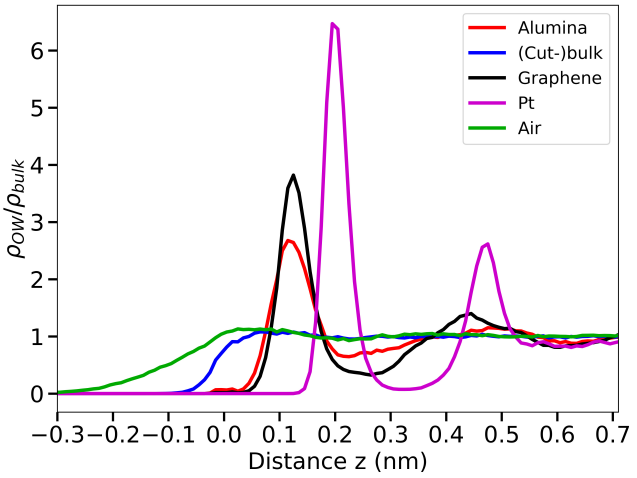

FIG. 2. Density profile (normalized to bulk water) of interfacial water molecules at the five surfaces studied in this work. "Distance z" represents the distance between water and the instantaneous surfaces. The left and right sides represent surface and bulk directions, respectively.

Another characteristic of a perfect 2D H-bond network is that all H-bonds are flat and parallel to the surface, which can be assessed using the probability distribution of H-bond orientations. In bulk water, H-bonds exhibit no preferred orientation, allowing their network to expand into all three dimensions. Conversely, H-bond networks tend to expand parallel rather than perpendicular to the surfaces. The distribution of H-bond orientation (Fig. 3a and b), $P(cos\phi, z)$, of interfacial water shows that near the cut-bulk surface (Fig. 3d), the count of H-bonds perpendicular to the surface diminishes. This decline can be attributed to the removal of water beyond the surface, along with the associated cross-surface H-bonds, which are likely oriented perpendicular to the surface. As the reference "surface", if there are more parallel H-bonds at other surfaces than cut-bulk, such H-bond network is considered as reduced dimensionality.

The H-bond network at the water/air interface is not isolated, as indicated by a distinct area within $|cos\phi| < 0.5$ and a thickness less than 0.2 nm (Fig. 3f). The observation suggests that interfacial waters remain connected with bulk water, even though a higher number of H-bonds exist within the first layer at $0.2 < z < 0.3$ nm compared to bulk water. At the alumina, graphene and Pt(111) surfaces that are characterized by higher local density, a significant number of H-bonds parallel to the surfaces are observed, making the $P(cos\phi, z)$ show a "K" pattern (Fig. 3). These interfacial H-bonds are flatter ($|cos\phi| < 0.4$) than those at the water/air interface and the thickness of the H-bond network is only about 0.1 nm as a result of high water local density that forces waters to form flat H-bonds. Similar behaviors have been observed for ions under 2D confinement, which tend to be paired, forming a crystal rather than a solution[51]. The H-bond density in the region $0.2 < z < 0.4$ nm for both $P(cos\phi, z)$ and $P(cos\phi|z)$ show the trend Pt > graphene > alumina (Fig. 3 and S2), indicating pronounced H-bond network isolation. That is, waters in this layer prefer H-bonds within the layer rather than other layers. This phenomenon occurs at the Pt surface and is the weakest at the alumina surface, consistent with their local water density. At all surfaces in this work, H-bond networks of interfacial waters that display behaviors of reduced dimensionality, such as parallel orientational and low density of interlayer H-bonds, are observed with an increased water local density.

Topology of interfacial H-bond networks

Universal enhanced connectivity and reduced dimensionality

The whole H-bond network also shows characteristics of reduced dimensionality. To assess the network connectivity quantitatively, the "maximum connected ratio" (MCR) is introduced as the ratio between the size of the maximum connected component and the number of interfacial waters:

$$MCR = \frac{N_{MCC}}{N} \quad (1)$$

where N represents the number of waters. The highest possible value of MCR is 1, when all interfacial waters are completely connected. The water 2D density (number of water per nm^2) is chosen as the independent variable

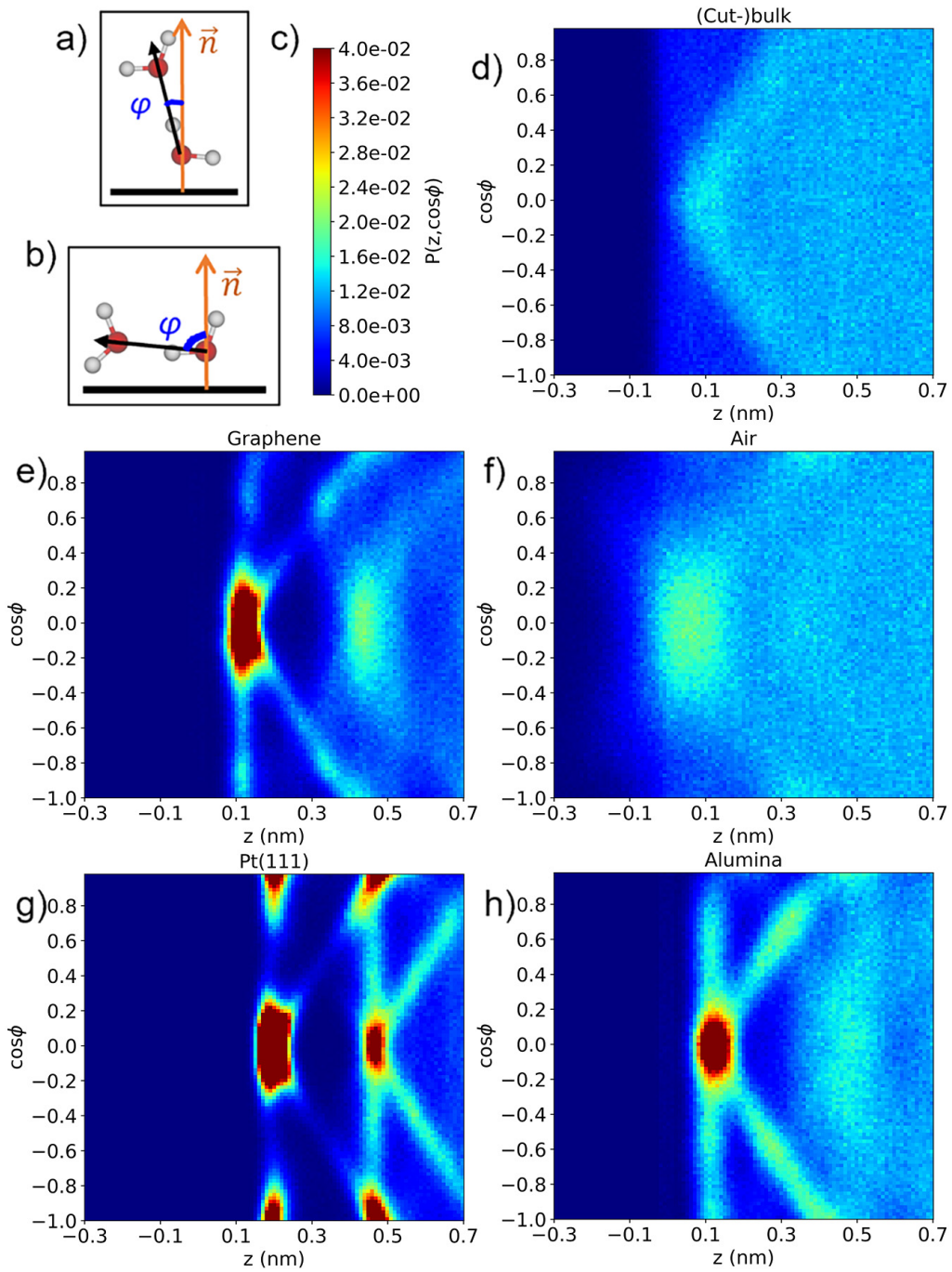

FIG. 3. Distribution of H-bond orientations of interfacial waters. a), b) Definition of the H-bond orientation angle; more details are discussed in SI. d)-h) Joint probability $P(cos\phi, z)$ for the five surfaces. The label z of x axes represents the distance between a water molecule and the instantaneous surface.

and it is correlated with the thickness of the water slab (Fig. S3). Even in bulk water, increasing the thickness of water slab or the water number 2D density results in a higher MCR value, consistent with the fact that in bulk water nearly all waters are connected via H-bonds. To eliminate the influence of small, isolated clusters, we adopt MCR = 0.95, i.e., when 95% of waters are connected in the H-bond network, is chosen as the threshold as connected. Comparing to the cut-bulk surface, fewer waters per unit area are required to reach connected at all other surfaces, in other words, each water occupies the larger space in the 2D plane.

The graphene and Pt(111) surfaces, characterized by high local water density, require the fewest waters to be

connected, displaying the most pronounced 2D characteristics. The 2D behavior near the alumina surface appears considerably weaker. In contrast to other surfaces that lack surface-water H-bonds, waters donate strong H-bonds to aluminol groups, which compete with water-water H-bonds, making water orientation perpendicular to the surface and disrupting the 2D behavior of interfacial H-bond network (Fig. 4)[42]. Based on these observations, 2D behaviors of H-bond networks are determined by two key factors. First, weak interactions between interfacial water and a surface promote 2D behaviors of the H-bond network, due to the challenging maintenance of a 3D H-bond network without water-surface H-bonds; as waters do not prefer free OH groups[52]. Second, water adsorption at surfaces increases the local density, forcing waters to be connected via internal H-bonds.

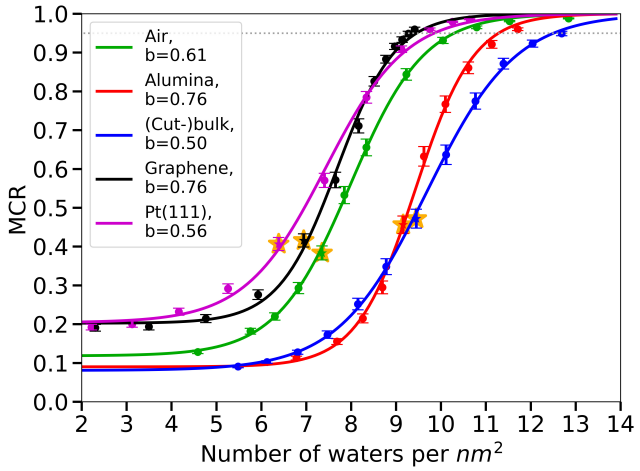

FIG. 4. The maximum connected component (MCR) value versus number of waters per nm^2 for all surfaces investigated. The gray dotted line at the top is MCR = 0.95, the threshold of a fully connected water slab. All other colored markers are directly calculated from simulation trajectories and all curves are fit using Eq. 2. Yellow star markers represent the critical percolation points.

The dimensionality can be effectively characterized using a metric that captures the rate at which H-bond networks expand in the third dimension. The speed of MCR growth is fit using:

$$y = a * tanh(b * x + c) + 1 - a \tag{2}$$

where the coefficient b describes the growth rate of MCR. Among all surfaces, the b value of cut-bulk is the smallest, consistent with the 3D behavior of bulk water. The MCR at other surfaces grows significantly faster than bulk water except for the Pt(111) surface whose low growth is attributed to the high local water density. When fitting the MCR to the thickness of H-bond networks, growth at the Pt(111) surface is the fastest among all surfaces and that of bulk water is still the lowest (Fig. S3). Although the b value alone is not a perfect indicator of the 2D behavior of networks, it offers indirect evidence for enhanced 2D behaviors for these surfaces.

Universal critical points of connectivity percolation transition

We also observed 2D percolation behaviors at all interfaces and a uniform percolation critical point in Fig. 4. At the critical point, we expected the power law of the probability distribution ($P(n)$) of the sizes of water clusters (n) to follow:

$$P(n) \sim n^{-\tau}, \tag{3}$$

where $\tau = 187/91 \approx 2.055$ is the two dimension critical Fisher exponent [53, 54]. For each thickness at each surface, we compute $P(n)$ and perform linear regression between $logP(n)$ and $logn$. The Pearson correlation coefficients (R^2) for all surfaces (Fig. S5) show that at very low thickness, a high R^2 is observed because there are not many water molecules. The exponential cut-off correction is expected to be significant only when n is high. The largest cluster sizes at these thickness are on the order of a dozen and are less by an order of magnitude compared to those at the critical percolation points, as shown in plots $P(n)$ with n for each thickness (Fig. S10 - S14). As a result, instead of selecting the maximum R^2, in this work, the thinnest water slab with $R^2 < 0.95$ is chosen as the critical point for each surface. Further increasing the thickness of water slabs leads to a rapid decrease in R^2. This sharp change in the behavior of R^2 is another piece of evidence that the percolation phase transition occurs at these points. R^2 continues to decrease with increased thickness because, above the percolation threshold, large clusters contains most water molecules are observed, resulting in a bimodal distribution of $P(n)$. At these points, all τ values obtained from Eq. 3 are around 2, consistent with the two dimensional critical Fisher exponent [54]. Last, the percolation critical points occur at about MCR=0.4 (Fig. 4) for all interfaces and we believe that it is a uniform behaviour of 2D H-bond network of interfacial water.

Enhanced connectivity slows down dynamics

The dynamics of interfacial water is also compared (Fig. S8). The interfacial region is divided into 4 layers by the distance to surfaces (defined in Table S3). In this work, the mean square displacement (MSD) on x and y directions is applied to describe water dynamics parallel to surfaces (Eq. 4)

$$MSD_{2d}(t) = \langle |(x(t) - x(0)|^2 + |y(t) - y(0)|^2) \rangle \tag{4}$$

In these calculations, the layers of water molecules are determined by their initial positions. The MSD data reveals that at layer 0 and layer 1, water dynamics are

TABLE I. τ values and thicknesses (nm) at each surface at the critical point.

Surface	Air	Alumina	(Cut-)bulk	Graphene	Pt(111)
Thickness	0.12	0.24	0.26	0.15	0.205
τ	1.894	1.575	1.638	1.733	1.811

faster at water/air interfaces but slower at other solid surfaces, because surface-water interactions restrict the movement of water molecules, whereas there is no such interaction between water and vacuum. The water dynamics at cut-bulk surfaces are the same at all layers because removing waters on one side after simulations for analysis does not affect the movement of individual water molecules. At solid interfaces, layers 2 and 3 are less affected by solid surfaces. Diffusion in the two layers are similar and comparable with the bulk. The continuous water residence autocorrelation function describes the movement of water perpendicular to surfaces,[42] and is defined by:

$$R(t) = \frac{\langle r(0)r(t)s_r(t)\rangle}{\langle r(0)r(0)\rangle} \tag{5}$$

$$s_r(t) = \prod_{i=0}^{t} r(i), \tag{6}$$

r(t) could be 1 or 0, representing whether a water molecule is in or out of a specific layer, respectively. R(t) exhibits a similar trend as shown 2D MSD: water molecules that move faster parallel to surfaces also do so perpendicularly. The only exception is the layer 2 at the water/Pt interface, where R(t) decays slower and close to layer 1 instead of layer 3 at other solid interfaces. Also, only layer 0 at water/air interface contains enough number of water molecules. At the solid surface, the layer is thin and cannot hold water. There is no water observed at layer 0 for the Pt surface.

CONCLUSION

In summary, we explored the topology of H-bond networks at the air, α-alumina(0001), modified graphene, and Pt(111) surfaces and compared them with the cut-bulk surface as a model of a 3D H-bond network. All surfaces show similar dimensionality, though it can take several nanometers for the intrinsic dimension to converge to the bulk value. In addition, at all surfaces compared to the cut-bulk, interfacial waters exhibit more H-bonds parallel to the surfaces. Using MCR and MCR growth as the metric of connectivity, we find that H-bond networks at all other surfaces need fewer waters to reach a connected graph, showing the increased connectivity and reduced dimensionality at interfaces. Surfaces with higher local water density and lower hydrophilicity show a more substantial reduction of dimensionality. Notably, the methodology we developed is not limited to planar surfaces and can be applied to water/protein and other soft surfaces. This adaptability allows for the exploration of interfacial H-bond networks and how the networks affect the chemistry and physics at the surfaces. In addition, developing advanced graph based models to describe interfacial water is also necessary to understand the structure and dynamics of phase transition of liquid water[39, 55].

ACKNOWLEDGEMENT

This work was supported as part of the Center for Complex Materials from First Principles (CCM), an Energy Frontier Research Center funded by the U.S. Department of Energy, Office of Science, Basic Energy Sciences under Award #DE-SC0012575. This research includes calculations carried out on HPC resources supported in part by the National Science Foundation through major research instrumentation Grant No. 1625061 and by the US Army Research Laboratory under contract number W911NF-16-2-0189.

* eborguet@temple.edu
† vincenzo.carnevale@temple.edu

[1] O. Björneholm, M. H. Hansen, A. Hodgson, L.-M. Liu, D. T. Limmer, A. Michaelides, P. Pedevilla, J. Rossmeisl, H. Shen, G. Tocci, E. Tyrode, M.-M. Walz, J. Werner, and H. Bluhm, Water at interfaces, Chemical Reviews **116**, 7698 (2016).
[2] J. Xu, M. Chen, C. Zhang, and X. Wu, First-principles study of the infrared spectrum in liquid water from a systematically improved description of h-bond network, Physical Review B **99**, 205123 (2019).
[3] R. Mu, Z.-j. Zhao, Z. Dohnálek, and J. Gong, Structural motifs of water on metal oxide surfaces, Chemical Society Reviews **46**, 1785 (2017).
[4] R. Wang, M. L. Klein, V. Carnevale, and E. Borguet, Investigations of water/oxide interfaces by molecular dynamics simulations, WIREs Computational Molecular Science **11**, e1537 (2021).
[5] J. L. Bañuelos, E. Borguet, J. Brown, Gordon E., R. T. Cygan, J. J. DeYoreo, P. M. Dove, M.-P. Gaigeot, F. M. Geiger, J. M. Gibbs, V. H. Grassian, A. G. Ilgen, Y.-S. Jun, N. Kabengi, L. Katz, J. D. Kubicki, J. Lützenkirchen, C. V. Putnis, R. C. Remsing, K. M. Rosso, G. Rother, M. Sulpizi, M. Villalobos, and H. Zhang, Oxide- and silicate-water interfaces and their

roles in technology and the environment, Chemical Reviews **123**, 6413 (2023).
[6] S. M. Piontek and E. Borguet, Vibrational spectroscopy of geochemical interfaces, Surface Science Reports , 100606 (2023).
[7] P. Xu, R. Wang, H. Zhang, V. Carnevale, E. Borguet, and J. Suntivich, Cation modifies interfacial water structures on platinum during alkaline hydrogen electrocatalysis, J. Am. Chem. Soc. **146**, 2426 (2024).
[8] C. Penschke, J. Thomas, C. Bertram, A. Michaelides, K. Morgenstern, P. Saalfrank, and U. Bovensiepen, Hydration at highly crowded interfaces, Phys. Rev. Lett. **130**, 106202 (2023).
[9] N. Di Pasquale, A. R. Finney, J. D. Elliott, P. Carbone, and M. Salvalaglio, Constant chemical potential–quantum mechanical–molecular dynamics simulations of the graphene–electrolyte double layer, The Journal of Chemical Physics **158** (2023).
[10] A. Luzar and D. Chandler, Hydrogen-bond kinetics in liquid water, Nature **379**, 55 (1996).
[11] Z. A. Piskulich, D. Laage, and W. H. Thompson, On the role of hydrogen-bond exchanges in the spectral diffusion of water, The Journal of Chemical Physics **154**, 064501 (2021).
[12] R. Wang, V. Carnevale, M. L. Klein, and E. Borguet, First-principles calculation of water pka using the newly developed scan functional, The Journal of Physical Chemistry Letters **11**, 54 (2020).
[13] P. L. Geissler, C. Dellago, D. Chandler, J. Hutter, and M. Parrinello, Autoionization in liquid water, Science **291**, 2121 (2001).
[14] A. Hassanali, F. Giberti, J. Cuny, T. D. Kuhne, and M. Parrinello, Proton transfer through the water gossamer, Proceedings of the National Academy of Sciences **110**, 13723 (2013).
[15] V. Quaranta, M. Hellström, and J. Behler, Proton-transfer mechanisms at the water-zno interface: The role of presolvation, The Journal of Physical Chemistry Letters **8**, 1476 (2017).
[16] S. Di Pino, Y. Perez Sirkin, U. N. Morzan, V. M. Sanchez, A. Hassanali, and D. A. Scherlis, Water self-dissociation is insensitive to nanoscale environments, Angewandte Chemie International Edition , e202306526 (2023).
[17] D. Muñoz Santiburcio and D. Marx, Nanoconfinement in slit pores enhances water self-dissociation, Phys. Rev. Lett. **119**, 056002 (2017).
[18] M. Calegari Andrade, R. Car, and A. Selloni, Probing the self-ionization of liquid water with ab initio deep potential molecular dynamics, Proceedings of the National Academy of Sciences **120**, e2302468120 (2023).
[19] R. Kumar, J. R. Schmidt, and J. L. Skinner, Hydrogen bonding definitions and dynamics in liquid water, The Journal of Chemical Physics **126**, 204107 (2007).
[20] M. K. Horton and M. A. Moram, Alloy composition fluctuations and percolation in semiconductor alloy quantum wells, Applied Physics Letters **110**, 162103 (2017).
[21] A. Geiger, F. H. Stillinger, and A. Rahman, Aspects of the percolation process for hydrogen-bond networks in water, The Journal of Chemical Physics **70**, 4185 (1979).
[22] S. Naserifar and W. A. Goddard III, Liquid water is a dynamic polydisperse branched polymer, Proceedings of the National Academy of Sciences **116**, 1998 (2019).
[23] R. L. Blumberg, H. E. Stanley, A. Geiger, and P. Mausbach, Connectivity of hydrogen bonds in liquid water, The Journal of Chemical Physics **80**, 5230 (1984).
[24] F. Tang, T. Ohto, S. Sun, J. R. Rouxel, S. Imoto, E. H. G. Backus, S. Mukamel, M. Bonn, and Y. Nagata, Molecular structure and modeling of water-air and ice-air interfaces monitored by sum-frequency generation, Chemical Reviews **120**, 3633 (2020).
[25] M. Bonn, Y. Nagata, and E. H. G. Backus, Molecular structure and dynamics of water at the water-air interface studied with surface-specific vibrational spectroscopy, Angewandte Chemie International Edition **54**, 5560 (2015).
[26] T. Ohto, M. Dodia, J. Xu, S. Imoto, F. Tang, F. Zysk, T. D. Kuhne, Y. Shigeta, M. Bonn, X. Wu, and Y. Nagata, Accessing the accuracy of density functional theory through structure and dynamics of the water-air interface, The Journal of Physical Chemistry Letters **10**, 4914 (2019).
[27] A. Serva, S. Pezzotti, S. Bougueroua, D. R. Galimberti, and M.-P. Gaigeot, Combining ab-initio and classical molecular dynamics simulations to unravel the structure of the 2d-hb-network at the air-water interface, Journal of Molecular Structure **1165**, 71 (2018).
[28] S. Pezzotti, A. Serva, F. Sebastiani, F. S. Brigiano, D. R. Galimberti, L. Potier, S. Alfarano, G. Schwaab, M. Havenith, and M.-P. Gaigeot, Molecular fingerprints of hydrophobicity at aqueous interfaces from theory and vibrational spectroscopies, The Journal of Physical Chemistry Letters **12**, 3827 (2021).
[29] A. Tuladhar, S. Dewan, S. Pezzotti, F. S. Brigiano, F. Creazzo, M.-P. Gaigeot, and E. Borguet, Ions tune interfacial water structure and modulate hydrophobic interactions at silica surfaces, Journal of the American Chemical Society **142**, 6991 (2020).
[30] A. Oleinikova, I. Brovchenko, N. Smolin, A. Krukau, A. Geiger, and R. Winter, Percolation transition of hydration water: From planar hydrophilic surfaces to proteins, Physical Review Letters **95**, 247802 (2005).
[31] M.-C. Bellissent-Funel, A. Hassanali, M. Havenith, R. Henchman, P. Pohl, F. Sterpone, D. van der Spoel, Y. Xu, and A. E. Garcia, Water determines the structure and dynamics of proteins, Chemical Reviews **116**, 7673 (2016).
[32] A. Arsiccio, J. McCarty, R. Pisano, and J.-E. Shea, Heightened cold-denaturation of proteins at the ice-water interface, Journal of the American Chemical Society **142**, 5722 (2020).
[33] S. Pezzotti, D. R. Galimberti, and M.-P. Gaigeot, 2d h-bond network as the topmost skin to the air-water interface, The Journal of Physical Chemistry Letters **8**, 3133 (2017).
[34] J.-H. Choi, H. Lee, H. R. Choi, and M. Cho, Graph theory and ion and molecular aggregation in aqueous solutions, Annual Review of Physical Chemistry **69**, 125 (2018).
[35] B. L. Mooney, L. R. Corrales, and A. E. Clark, Molecularnetworks: An integrated graph theoretic and data mining tool to explore solvent organization in molecular simulation, Journal of Computational Chemistry **33**, 853 (2012).
[36] J.-H. Choi and M. Cho, Ion aggregation in high salt solutions. ii. spectral graph analysis of water hydrogen-bonding network and ion aggregate structures, The Journal of Chemical Physics **141**, 10.1063/1.4897638 (2014).

[37] J.-H. Choi and M. Cho, Ion aggregation in high salt solutions. vi. spectral graph analysis of chaotropic ion aggregates, The Journal of Chemical Physics **145**, 10.1063/1.4966246 (2016).
[38] S. Sundar, A. A. Sandilya, and M. H. Priya, Unraveling the influence of osmolytes on water hydrogen-bond network: From local structure to graph theory analysis, Journal of Chemical Information and Modeling **61**, 3927 (2021).
[39] F. M. Dietrich, X. R. Advincula, G. Gobbo, M. A. Bellucci, and M. Salvalaglio, Machine learning nucleation collective variables with graph neural networks, Journal of Chemical Theory and Computation **20**, 1600 (2024).
[40] See supplemental material at [url will be inserted by publisher] for simulation settings and additional analysis.
[41] M. J. DelloStritto, S. M. Piontek, M. L. Klein, and E. Borguet, Effect of Functional and Electron Correlation on the Structure and Spectroscopy of the Al2O3(001)-H2O Interface, The Journal of Physical Chemistry Letters **10**, 2031 (2019).
[42] R. Wang, Y. Zou, R. C. Remsing, N. O. Ross, M. L. Klein, V. Carnevale, and E. Borguet, Superhydrophilicity of α-alumina surfaces results from tight binding of interfacial waters to specific aluminols, Journal of Colloid and Interface Science **628**, 943 (2022).
[43] J. D. Cyran, M. A. Donovan, D. Vollmer, F. Siro Brigiano, S. Pezzotti, D. R. Galimberti, M.-P. Gaigeot, M. Bonn, and E. H. G. Backus, Molecular hydrophobicity at a macroscopically hydrophilic surface, Proceedings of the National Academy of Sciences **116**, 1520 (2019).
[44] C. Wang, H. Lu, Z. Wang, P. Xiu, B. Zhou, G. Zuo, R. Wan, J. Hu, and H. Fang, Stable liquid water droplet on a water monolayer formed at room temperature on ionic model substrates, Physical Review Letters **103**, 137801 (2009).
[45] P. Grassberger and I. Procaccia, Measuring the strangeness of strange attractors, Physica D: Nonlinear Phenomena **9**, 189 (1983).
[46] D. Granata and V. Carnevale, Accurate estimation of the intrinsic dimension using graph distances: Unraveling the geometric complexity of datasets, Scientific Reports **6**, 31377 (2016).
[47] A. P. Willard and D. Chandler, Instantaneous liquid interfaces, The Journal of Physical Chemistry B **114**, 1954 (2010).
[48] R. Ma, D. Cao, C. Zhu, Y. Tian, J. Peng, J. Guo, J. Chen, X.-Z. Li, J. S. Francisco, X. C. Zeng, L.-M. Xu, E.-G. Wang, and Y. Jiang, Atomic imaging of the edge structure and growth of a two-dimensional hexagonal ice, Nature **577**, 60 (2020).
[49] V. Kapil, C. Schran, A. Zen, J. Chen, C. J. Pickard, and A. Michaelides, The first-principles phase diagram of monolayer nanoconfined water, Nature **609**, 512 (2022).
[50] J. Jiang, Y. Gao, W. Zhu, Y. Liu, C. Zhu, J. S. Francisco, and X. C. Zeng, First-principles molecular dynamics simulations of the spontaneous freezing transition of 2d water in a nanoslit, J. Am. Chem. Soc. **143**, 8177 (2021).
[51] W. Zhao, Y. Sun, W. Zhu, J. Jiang, X. Zhao, D. Lin, W. Xu, X. Duan, J. S. Francisco, and X. C. Zeng, Two-dimensional monolayer salt nanostructures can spontaneously aggregate rather than dissolve in dilute aqueous solutions, Nature Communications **12**, 5602 (2021).
[52] T. Sato, T. Sasaki, J. Ohnuki, K. Umezawa, and M. Takano, Hydrophobic surface enhances electrostatic interaction in water, Phys. Rev. Lett. **121**, 206002 (2018).
[53] S. Fayfar, A. Bretaña, and W. Montfrooij, Protected percolation: a new universality class pertaining to heavily-doped quantum critical systems, Journal of Physics Communications **5**, 015008 (2021).
[54] A. Suma, D. Sigg, S. Gallagher, G. Gonnella, and V. Carnevale, Ion channels in critical membranes: Clustering, cooperativity, and memory effects, PRX Life **2**, 013007 (2024).
[55] M. Farshad, M. J. DelloStritto, A. Suma, and V. Carnevale, Detecting liquid–liquid phase separations using molecular dynamics simulations and spectral clustering, The Journal of Physical Chemistry B **127**, 3682 (2023).